

Characterization of photon counting pixel detectors based on semi-insulating GaAs sensor material

To cite this article: E Hamann *et al* 2013 *J. Phys.: Conf. Ser.* **425** 062015

View the [article online](#) for updates and enhancements.

Related content

- [Investigation of GaAs:Cr Timepix assemblies under high flux irradiation](#)
E. Hamann, T. Koenig, M. Zuber *et al.*
- [The LAMBDA photon-counting pixel detector and high-Z sensor development](#)
D Pennicard, S Smoljanin, B Struth *et al.*
- [Properties of GaAs:Cr-based Timepix detectors](#)
P. Smolyanskiy, B. Bergmann, G. Chelkov *et al.*

Recent citations

- [Homogeneity study of a GaAs:Cr pixelated sensor by means of X-rays](#)
T. Billoud *et al*
- [Properties of GaAs:Cr-based Timepix detectors](#)
P. Smolyanskiy *et al*
- [Characterization of chromium compensated GaAs as an X-ray sensor material for charge-integrating pixel array detectors](#)
J. Becker *et al*



IOP | ebooks™

Bringing you innovative digital publishing with leading voices to create your essential collection of books in STEM research.

Start exploring the collection - download the first chapter of every title for free.

Characterization of photon counting pixel detectors based on semi-insulating GaAs sensor material

E Hamann^{1,2}, A Cecilia^{1,2}, A Zwerger², A Fauler², O Tolbanov³, A Tyazhev³, G Shelkov⁴, H Graafsma⁵, T Baumbach¹ and M Fiederle^{1,2}

¹IPS, Karlsruhe Institute of Technology, 76344 Eggenstein-Leopoldshafen, Germany

²FMF, Albert-Ludwigs-Universitaet Freiburg, 79104 Freiburg, Germany

³Tomsk State University, Tomsk, Russia

⁴JINR, Dubna, Russia

⁵DESY, Hamburg, Germany

E-mail: elias.hamann@kit.edu

Abstract. Hybrid semiconductor pixel detectors are considered of high interest for synchrotron applications like diffraction and imaging experiments. However, at photon energies above 30 keV, high-Z sensor materials have to be used due to the weak absorption of the most commonly used sensor material, for instance silicon wafers with a thickness of a few hundred μm . Besides materials like CdTe and Ge, semi-insulating, chromium compensated SI-GaAs(Cr) proves to be a promising sensor material for applications with X-rays in the mid-energy range up to ~ 60 keV. In this work, material characterisation of SI-GaAs(Cr) wafers by electrical measurements and synchrotron white beam topography as well as the characterization and application of pixel detector assemblies based on Medipix readout chips bump-bonded to 500 μm thick SI-GaAs(Cr) sensors are presented. The results show a very homogeneous material with high resistivity and good electrical properties of the electrons as well as a very promising imaging performance of the detector assemblies.

1. Introduction

For many synchrotron applications, e.g. for scattering and imaging experiments, photon counting direct converting semiconductor pixel detectors have become a well established alternative to classical scintillator/optics/CCD based synchrotron cameras when highest spatial resolution in the μm -range is not needed. These detectors offer large active areas of several cm^2 , high sensitivity, a high dynamic range by setting energy thresholds above the electronic noise level and high frame rates.

The most commonly used sensor material for X-ray detection is silicon with a thickness of several hundreds of micrometers, due to the availability of relatively cheap wafers which show highly homogeneous crystal and electrical properties over large areas.

However, the use of silicon is limited to photon energies below 30 keV by its low atomic number ($Z=14$) and the subsequent low absorption efficiency for higher photon energies. Therefore, materials showing higher atomic numbers, like CdTe ($Z=48, 52$) or Ge ($Z=32$) have to be used. As shown previously [1], semi-insulating (SI), chromium (Cr) compensated GaAs ($Z=31, 33$) also proves to be a good alternative as sensor material for detection of X-rays in the mid-energy range up to ~ 60 -80 keV, closing the gap between the low-absorbing, high quality Si and the high absorbing, lower quality CdTe.

In this work, SI-GaAs(Cr) wafers were characterized with respect to resistivity and electrical properties of the electrons as well as by synchrotron radiation white beam topography. Detector assemblies based on Timepix readout chips bump-bonded to GaAs sensors were fabricated and characterized with a microfocus X-ray tube. All measurements were performed at room temperature.

2. Timepix detector

The Timepix readout chip [2] has a matrix of 256×256 square pixels with a 55 μm pitch, covering an active area of 1.98 cm^2 . Each pixel contains a charge sensitive preamplifier, a threshold discriminator

circuit and a 14-bit pseudo-random counter. Pixel-to-pixel variations in the globally set energy threshold can be minimized by a 4-bit digital-to-analog-converter (DAC) in every pixel.

The Timepix chip can be set to work in electron or hole collection mode and is capable to compensate for leakage currents from the sensor material up to 10 nA/pixel (electron collection) or 20 nA/pixel (hole collection). The Timepix chip is buttable on three sides which allows to increase the active area by bump-bonding larger sensor crystals to a $2 \times N$ matrix of readout chips.

3. GaAs sensor material

In contrast to epitaxial layers, the semi-insulating GaAs sensor material used in this work was produced by thermal diffusion of chromium into LEC-grown n-type 40 mm diameter GaAs wafers at the Tomsk State University [3]. After polishing, the resulting thickness of the wafers was 500 μm .

The processed and diced sensors then were bump-bonded to the readout chip by a low temperature flip-chip process at the FMF Freiburg. The planar backside metal contact, on which the bias voltage was applied, consisted of 1 μm Ni; no guard-rings were applied on either side of the sensor. The GaAs Timepix detectors were operated with negative bias, thus collecting electrons in the pixels.

4. Results and Discussion

4.1. Electrical properties of GaAs(Cr) wafers

The resistivity of the 40 mm diameter SI-GaAs(Cr) wafers and the mobility-lifetime ($\mu\tau$) product of the electrons were determined by a combined contactless resistivity and mu-tau mapping device [4] using the time domain charge measurement (TDCM) technique [5] and laser pulses, respectively. The wafer under investigation showed resistivity values up to $3 \times 10^9 \Omega\text{cm}$, the higher values were measured in the upper part of the wafer. The $\mu\tau$ product of the electrons was found to be around $1 \times 10^{-3} \text{ cm}^2/\text{V}$ homogeneously across the wafer; only the values at the very edge of the wafer (the outermost 2-3 mm) were considerably lower.

Although the scanning steps were too large to resolve local variations of the $\mu\tau$ product in the (sub-)mm regime [6], these results show very good electrical properties of the electrons in SI-GaAs(Cr), being about one order of magnitude higher compared to literature, e.g. [7].

4.2. Synchrotron radiation white beam topography

In order to qualitatively investigate the crystal properties of SI-GaAs(Cr), synchrotron radiation white beam topography in back reflection mode was performed at the TOPO-TOMO beamline at the ANKA light source at KIT [8]. A $4 \times 4 \text{ mm}^2$ beam was scanned over an area of about $2 \times 2 \text{ cm}^2$ in the centre of the wafer. The resulting Laue pattern was recorded with high resolution photographic film (*Slavich VRP-M*) and the same reflex at each scan position was digitized using a low magnification microscope and a digital camera.

Figure 1 shows a stitched image of the 30 single topograms as well as a $4 \times 8 \text{ mm}^2$ large detail of the image. Besides a network of smaller dislocations typical of melt-grown GaAs, only very few large features which give rise to orientation contrast (larger dislocations, small angle grain boundaries etc.) are visible. The bright spots and scratches originate from dust and scratches on the photographic film.

4.3. Timepix detector assembly characterization

Two SI-GaAs(Cr) sensors were processed, diced and bump-bonded to Timepix readout chips. The leakage current of both sensors was measured as a function of the applied (negative) bias voltage in the range from 0 to -800 V, as shown in figure 2. Both assemblies showed almost exactly matching U-I dependences with a linear behaviour up to -400 V proving the resistive behaviour of the semi-insulating material.

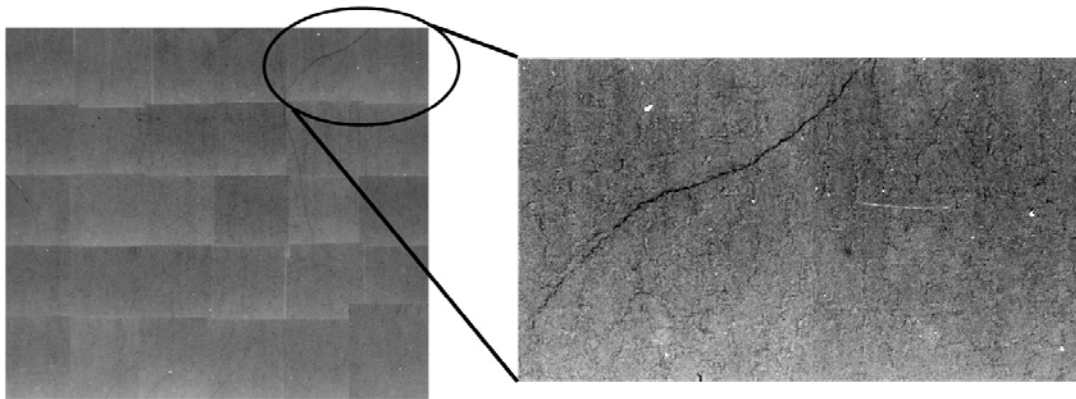


Figure 1. Synchrotron radiation white beam Topography of the SI-GaAs(Cr) wafer; stitching of 30 single acquisitions (left) and zoomed 4×8 mm² detail (right).

For higher bias voltages, the leakage current increased superlinearly. Linear fits from 0 to -400 V show a total resistivity of the assemblies of $2.7 \times 10^7 \Omega$, which is a factor of ~ 2.5 lower than calculated from the bulk resistivity values from section 4.1. However, due to the absence of a guard-ring, a large part of the leakage current is believed to flow along the dicing edge of the sensor which could explain this factor, along with possible charge carrier injection after processing/contact deposition.

Figure 3 shows a flood image of one of the detector assemblies acquired at -400 V bias using a commercial microfocus X-ray tube (W target). The acceleration voltage was set to 80 kVp and the tube current to 500 μA . The total bonding yield is found to be 99.9%.

The count rate variations in the flood image illustrate the typical dislocation cell structure of melt grown GaAs [9], leading to locally varying electric fields and charge carrier mobility. The diagonal line structures visible in the image are assumed to match the larger structures leading to the orientation contrast as shown in the topogram in figure 1. The bright (=higher counting) regions in the outermost parts of the image stem from pixels with high, but still compensated leakage current whereas in the dark (=non-counting) pixels the leakage current is too high to be compensated. This behaviour again confirms the above mentioned increased leakage current along the sensor edge.

For imaging purposes, however, applying a standard flatfield correction drastically increases the image quality and almost completely compensates the material inhomogeneities, as shown in figure 4. Here, a corrected X-ray image of an integrated circuit on a PCB is shown, acquired under the same parameters as the flood image in figure 3.

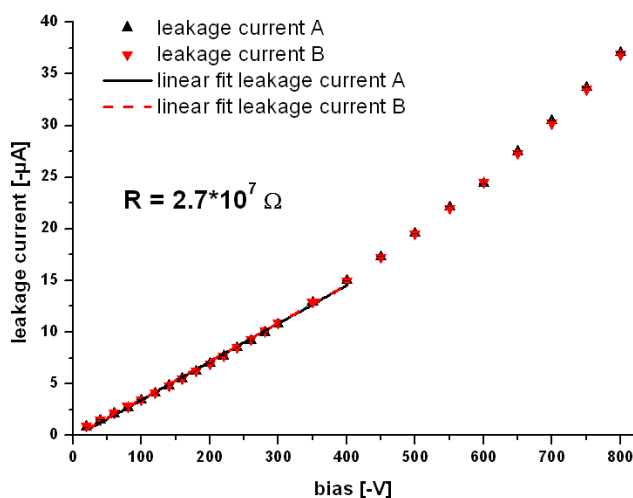


Figure 2. Leakage current vs. bias voltage for the two GaAs Timepix detector assemblies.

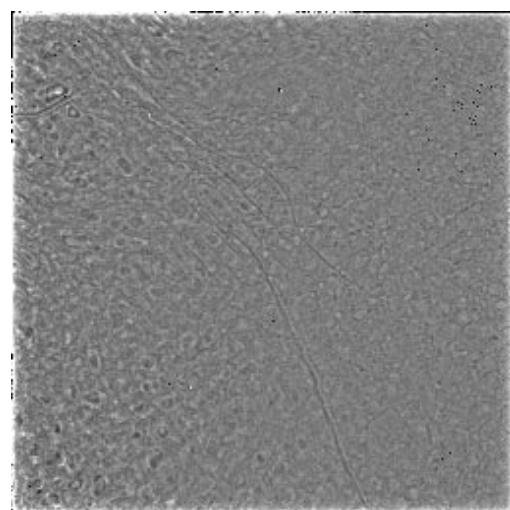


Figure 3. Flood image of a GaAs Timepix assembly.

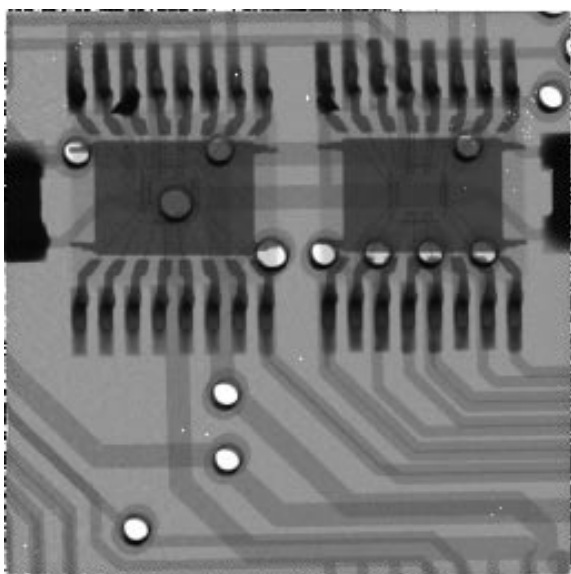


Figure 4. Flatfield corrected X-ray image of an integrated circuit on a PCB.

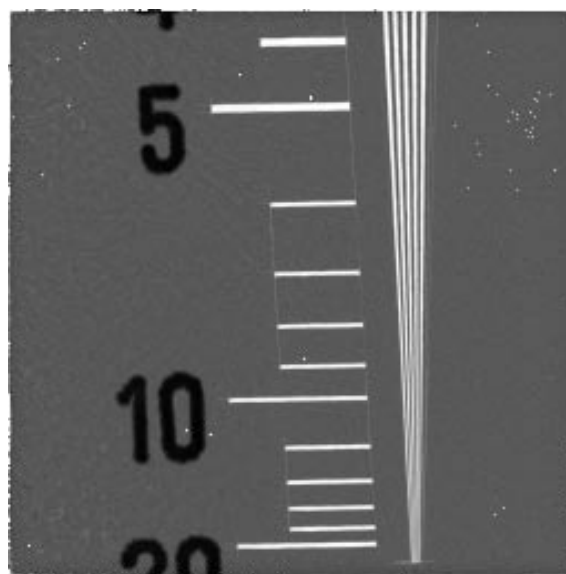


Figure 5. Flatfield corrected image of a lead test pattern for spatial resolution tests.

A qualitative analysis of the flatfield corrected image of a lead test pattern shown in figure 5 leads to a spatial resolution of ~ 8 lp/mm, a value close to the theoretical limit of 9.1 lp/mm imposed by the pixel size of $55 \mu\text{m}$ (Nyquist criterion).

5. Conclusions and outlook

The performance of SI-GaAs(Cr) for application as sensor material for hybrid semiconductor pixel detectors was shown. Wafer characterization revealed a high resistivity and comparably good charge carrier properties of the material. The crystal homogeneity of the wafer and absence of large defects was shown by synchrotron radiation white beam topography.

The characterization of two processed sensors, bump-bonded to Timepix readout chips, confirmed the resistive behavior of the sensor material and showed a very high bonding yield. Inherent count rate variations in X-ray images due to the cell structure of melt-grown GaAs can be compensated by simple flatfield correction leading to a very good image quality. The spatial resolution of the sensors was found to be close to the theoretical limit.

A deeper, quantitative analysis of other important parameters, like long-term stability of the sensors, the MTF and CCE as well as the response to monochromatic photons and the application of the sensors in synchrotron beamlines will be done in the near future. The implementation of guard-ring structures and the production of larger area detector assemblies are foreseen.

References

- [1] Tlustos L, Shelkov G and Tolbanov O 2011 *Nucl. Instr. and Meth. A* **633** 103-107
- [2] Llopart X, Ballabriga R, Campbell M, Tlustos L and Wong W 2007 *Nucl. Instr. and Meth. A* **581** 485-494
- [3] Ayzenshtat G et al. 2002 *Nucl. Instr. and Meth.* **494** 120-127
- [4] Sowinska M et al. 2011 *IEEE NSS/MIC/RTSD Conference record* 4829-4832
- [5] Stibal R et al. 1991 *Semicond. Sci. Technol.* **6** 995
- [6] Stibal R, Wickert M, Hiesinger P and Jantz W 1999 *Mat. Sc. and Eng. B* **66** 21-25
- [7] Sellin P 2003 *Nucl. Instr. and Meth. A* **513** 332-339
- [8] Danilewsky A, Simon R, Fauler A, Fiederle M, Benz K 2003 *Nucl. Instr. Meth. B* **199** 71-74
- [9] Rudolph P 2005 *Cryst. Res. Technol.* **40** 7-20